Article

Layer Structure Preservation during Swelling, Pillaring, and Exfoliation of a Zeolite Precursor

Sudeep Maheshwari, Edgar Jordan, Sandeep Kumar, Frank S. Bates, R. Lee Penn, Daniel F. Shantz, and Michael Tsapatsis

J. Am. Chem. Soc., **2008**, 130 (4), 1507-1516 • DOI: 10.1021/ja077711i

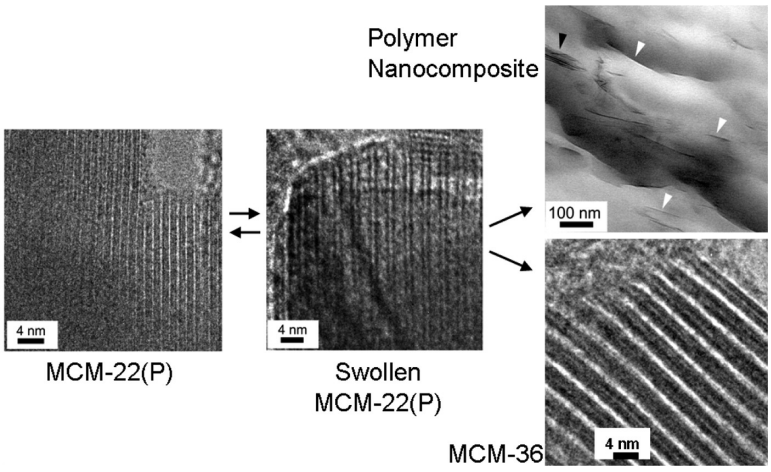

More About This Article

Additional resources and features associated with this article are available within the HTML version:

- Supporting Information
- Links to the 5 articles that cite this article, as of the time of this article download
- Access to high resolution figures
- Links to articles and content related to this article
- Copyright permission to reproduce figures and/or text from this article

View the Full Text HTML

J|A|C|S
ARTICLES
Published on Web 01/08/2008

Layer Structure Preservation during Swelling, Pillaring, and Exfoliation of a Zeolite Precursor

Sudeep Maheshwari,[†] Edgar Jordan,[‡] Sandeep Kumar,[†] Frank S. Bates,[†] R. Lee Penn,[§] Daniel F. Shantz,[‡] and Michael Tsapatsis*,[†]

Department of Chemical Engineering and Materials Science, University of Minnesota, Minneapolis, Minnesota 55455, Department of Chemical Engineering, Texas A&M University, College Station, Texas 77843, and Department of Chemistry, University of Minnesota, Minneapolis, Minnesota 55455

Received October 7, 2007; E-mail: tsapatsi@cems.umn.edu

Abstract: MCM-22(P), the precursor to zeolite MCM-22, consists of stacks of layers that can be swollen and exfoliated to produce catalytically active materials. However, the current swelling procedures result in significant degradation of crystal morphology along with partial loss of crystallinity and dissolution of the crystalline phase. Fabrication of polymer nanocomposites and coatings with MCM-22 for separation, barrier, and other applications requires a swelling method that does not alter drastically the crystal morphology and layer structure and preserves the high aspect ratio of the layers. Here, we demonstrate such a method by swelling MCM-22(P) at room temperature. The low-temperature process does not disrupt the framework connectivity present in the parent MCM-22(P) material. By extensive washing with water, the swollen material, MCM-22(PS-RT), evolves to a new ordered layered structure. Interestingly, the swelling procedure is reversible and the swollen material can be restored back to MCM-22(P) by acidification of the sample. The swollen material can also be pillared to produce an MCM-36 analogue. It can also be exfoliated, and layers can be incorporated in a polymer matrix to make nanocomposites.

1. Introduction

MCM-22[1] is one of the most interesting zeolite structures synthesized in the past decade. This is in part because it crystallizes in the form of a layered precursor, MCM-22(P), composed of 2.5 nm thick sheets stacked in registry.[2] Each sheet consists of a bidimensional 10-member ring (MR) sinusoidal channel pore system and large 12-MR cups on the crystal surface.[3] These large cups are connected to each other through double 6-MR. Upon calcination, the layers condense together to form a 3-D framework structure, MCM-22. However, the major interest in MCM-22(P) arises from the fact that the layers can be swollen, pillared, and exfoliated under suitable conditions to give a range of catalytically active materials for cracking and other applications. Kresge and co-workers[4−6] have demonstrated a method to swell MCM-22(P) layers by treatment with a base, tetrapropylammonium hydroxide (TPAOH), and a long chain surfactant, cetyl trimethyl ammonium bromide (CTAB), under high pH and elevated temperature conditions. The swollen material can subsequently be pillared to produce a catalytically active material, MCM-36, with a very high surface area. Corma and co-workers[7,8] used ultrasonication to force apart the layers of the swollen material to produce a delaminated zeolite material, ITQ-2, with further improvements in the catalytic activity. ITQ-2 contains exfoliated single crystalline layers with the pore structure of MCM-22(P) layers.

We are interested in making MCM-22 nanocomposites with polymer and sol−gel matrices for separation and barrier applications.[9,10] Delaminated high aspect ratio MCM-22 layers are promising for this purpose. Up to now, we fabricated composites of MCM-22 with polymers[10] and mesoporous silica.[9] The latter showed improved selectivity for hydrogen over carbon dioxide indicating the molecular sieving potential of MCM-22. Although MCM-22 crystals possessing plate-like morphology are relatively thin (∼100−200 nm) and have a high aspect ratio (∼10), it is desirable to further reduce the film thickness by exfoliation to single layers. The typical thickness of a single MCM-22 layer is about 2.5 nm, which, in principle, allows fabrication of membranes with thin permselective layers. In addition, appropriately oriented high aspect ratio delaminated layers are expected to enhance the permselectivity even at relatively small amounts (∼2−3 wt %).[11,12]

[†] Department of Chemical Engineering and Materials Science, University of Minnesota.
[‡] Texas A&M University.
[§] Department of Chemistry, University of Minnesota.

(1) Rubin, M. K.; Chu, P. U.S. Patent 4954325, 1990.
(2) Roth, W. J.; Vartuli, J. C. *Stud. Surf. Sci. Catal.* **2002**, *141*, 273−279.
(3) Ravishankar, R.; Bhattacharya, D.; Jacob, N. E.; Sivasanker, S. *Microporous Materials* **1995**, *4* (1), 83−93.
(4) Kresge, C. T.; Roth, W. J. U.S. Patent 5266541, 1993.
(5) Kresge, C. T.; Roth, W. J. U.S. Patent 5278115, 1994.
(6) Kresge, C. T.; Roth, W. J.; Simmons, K. G.; Vartuli, J. C. WO 9211935, 1992.
(7) Corma, A.; Fornes, V.; Martinez-Triguero, J.; Pergher, S. B. *J. Catal.* **1999**, *186* (1), 57−63.
(8) Corma, A.; Fornes, V.; Pergher, S. B.; Maesen, T. L. M.; Buglass, J. G. *Nature (London)* **1998**, *396* (6709), 353−356.
(9) Choi, J.; Lai, Z.; Ghosh, S.; Beving, D. E.; Yan, Y.; Tsapatsis, M. *Ind. Eng. Chem. Res.* **2007**, *46* (22), 7096−7106.
(10) Choi, S.; Coronas, J.; Lai, Z.; Yust, D.; Onorato, F.; Tsapatsis, M. *J. Membrane Sci*. **2007**, DOI:10.1016/j.memsci.2007.09.026, available online.

Fabrication of polymer nanocomposites with layered materials requires intercalation of polymer chains in between the layers. To facilitate the intercalation, layered materials (e.g., clays) are often swollen with organic surfactant to increase the interlayer spacing. The increased interlayer spacing allows intercalation of polymer chains resulting in nanocomposites with intercalated or exfoliated morphology.[13,14] Given that the swelling and exfoliation methods for MCM-22(P) are already well established[6,8] a polymer nanocomposite with exfoliated MCM-22 layers would seem straightforward. However, it has been recognized[3,15,16] that swelling of MCM-22(P) by treatment with TPAOH and CTAB at elevated temperature and high pH results in layer fragmentation along with partial dissolution of the framework silica. Schenkel et al.[15] have reported a significant reduction in Si/Al ratio as a result of swelling and exfoliation procedures due to dissolution of silica. Apparently, partial MCM-22(P) dissolution during high-temperature swelling does not prohibit catalytic uses as demonstrated by successful applications of ITQ-2[8,17] and MCM-36.[17−19] However, it can significantly compromise the performance of nanocomposite membranes as a reduction in the aspect ratio of the layers can impair the separation capabilities of the membrane. Moreover, the amorphous silica produced by the dissolution of crystals may have an undesirable influence over the transport and separation properties of the membrane and may also cause processing problems during nanocomposite fabrication (e.g., due to aggregation).

In this report, a modified approach to swell MCM-22(P) without disruption of the layered structure is described. Relatively mild conditions are used as compared to the high-temperature basic conditions employed in the reported swelling procedures.[4−8] The resulting swollen material is compared with one swollen at elevated temperature to highlight the structural differences in the two materials. Reversibility of the swelling process is demonstrated, which represents a major difference from high-temperature methods that yield irreversibly swollen products. In addition to providing a modified approach to swell MCM-22(P) layers, this work enhances our understanding of the swelling of MCM-22(P) and presents a possible mechanism for reversible swelling. The swollen material has been successfully pillared to produce an MCM-36 analogue. Also, nanocomposites of swollen MCM-22(P) with polystyrene exhibiting partially exfoliated morphology of layers are demonstrated.

2. Experimental Section

2.1. Synthesis of MCM-22(P). MCM-22(P) was synthesized using the method described by Corma et al.[7,8] Typically, 0.72 g of sodium aluminate (MP biomedicals, USA) and 2.48 g of sodium hydroxide (97+ %, Fisher) were dissolved in 311 g of distilled water. Subsequently, 19.1 g of hexamethyleneimine (HMI) (Aldrich) and 23.6 g of fumed silica (Cab-o-sil M5) were added to the mixture. The mixture was allowed to stir for 5 h at room temperature, followed by 11 days in rotating Teflon-lined steel autoclaves at 408 K. The crystalline product obtained after 11 days was collected by centrifugation and repeatedly washed with distilled water to reduce the pH to 9. A portion of the crystalline product was calcined at 540 °C under air for 12 h to produce MCM-22.

2.2. Swelling and Pillaring of MCM-22(P). MCM-22(P) was swollen with CTAB at room temperature under high pH conditions. The composition of the swelling mixture was the same as reported by Kresge[6] and Corma.[7,8] Typically 9.0 g of aqueous slurry of MCM-22-(P) (20 wt % solids) was mixed with 35.0 g of an aqueous solution of 29 wt % CTAB (Aldrich) and 11.0 g of an aqueous solution of 40 wt % TPAOH (Alfa Aesar). The pH of the resulting mixture was typically 13.80. The mixture was allowed to stir for 16 h at room temperature, after which the particles were recovered by repeated cycles of centrifugation and water washing (10 min centrifugation at 10 000 rpm, and redispersion in fresh water). The number of (centrifugation/water washing) cycles was systematically varied from 10 to 40 to study its effect on the recorded XRD patterns. A portion of the mixture, recovered after 16 h of swelling, was subjected to ultrasonication for 2 h using a Branson 5510 ultrasonic cleaner, to attempt exfoliation of the layers,[8] and subsequently acidified to pH < 2 to collect the particles. For comparison, a portion of MCM-22(P) was also swollen at elevated temperature (80 °C) following the procedure reported by Corma et al.[7,8]

Pillaring of the swollen material was performed according to the procedure reported by Barth et al.[20] Typically, 1.0 g of swollen MCM-22(P) powder was mixed with 5.0 g of TEOS (tetraethoxysilane, Fluka), stirred for 25 h at 351 K under an argon atmosphere, then filtered, and dried at room temperature. The dried solid (0.5 g) was hydrolyzed with water (5.0 g, pH ∼8, controlled with NaOH) for 6 h at 313 K, and then filtered, dried at 300 K, and calcined at 723 K under N_2 flow (140 mL min^{-1}) for 6 h and finally at 823 K under air for 12 h (temperature ramp rate of 2 K/min).

2.3. Polystyrene-Swollen MCM-22(P) Nanocomposite Fabrication. 2.3.1. Nanocomposite from Solution Casting Techniques. Nanocomposites of room-temperature swollen MCM-22(P) and polystyrene were prepared using solvent blending techniques. A 2 wt % dispersion of swollen MCM-22(P) was prepared in toluene. To assist homogeneous dispersion, the mixture was subjected to 10 cycles of sonication and refluxing (6 h sonication, 6 h refluxing). The resulting dispersion (1.0 g) was mixed with 1.0 g of 2 wt % polystyrene (M_n = 5400) solution in toluene and stirred for 5 days. Subsequently, the mixture was heated for 2 h at 110 °C, followed by addition of 5.0 g of 20 wt % solution of polystyrene (M_n = 45 000), further heating (2 h, 110 °C), sonication (1 h), and finally casting on a Teflon plate. The solvent was evaporated slowly over a period of 5 days, and the composite was peeled off the surface.

2.3.2. Nanocomposite from Melt Compounding Techniques. Nanocomposites were prepared by melt blending in a DACA Mini Compounder vertical, co-rotating twin screw extruder with a recirculation channel. Polystyrene (3.8 g, M_n = 45 000) and room-temperature swollen MCM-22(P) (0.16 g) were mixed manually and loaded into the compounder preheated to 120 °C. The mixture was blended sequentially at 120 °C for 10 min, 170 °C for 10 min, and 150 °C for 5 min and finally extruded out at 130 °C. A screw speed of 350 rpm and nitrogen environment was used for blending. A circular disc (25 mm × 1 mm) was prepared by compressing the extrudate at 1000 psi and 150 °C for 10 min.

2.4. Characterization Methods. The silicon and aluminum contents of MCM-22(P), and of the swollen materials, were determined using Inductive Couple Plasma Mass Spectroscopy (ICP-MS) analysis conducted at Galbraith Laboratories, USA.

(11) Cussler, E. L. *J. Membrane Sci.* **1990**, *52* (3), 275−88.
(12) Choi, S.; Coronas, J.; Jordan, E.; Oh, W.; Nair, S.; Onorato, F.; Shantz, D. F.; Tsapatsis, M. *Angew. Chem., Int. Ed.* **2007**, DOI 10.1002/anie.200703440, available online.
(13) Giannelis, E. P. *Adv. Mater.* (Weinheim, Germany) **1996**, *8* (1), 29−35.
(14) Ray, S. S.; Okamoto, M. *Prog. Polym. Sci.* **2003**, *28* (11), 1539−1641.
(15) Schenkel, R.; Barth, J. O.; Kornatowski, J.; Lercher, J. A. *Stud. Surf. Sci. Catal.* **2002**, *142A*, 69−76.
(16) Wu, P.; Nuntasri, D.; Ruan, J.; Liu, Y.; He, M.; Fan, W.; Terasaki, O.; Tatsumi, T. *J. Phys. Chem. B* **2004**, *108* (50), 19126−19131.
(17) Corma, A.; Diaz, U.; Fornes, V.; Guil, J. M.; Martinez-Triguero, J.; Creyghton, E. J. *J. Catal.* **2000**, *191* (1), 218−224.
(18) Chu, C. T.; Husain, A.; Huss, A., Jr.; Kresge, C. T.; Roth, W. J. U.S. Patent 5258569, 1993.
(19) Hellring, S. D.; Huss, A. Jr.; Landis, M. E.; Marler, D. O.; Teitman, G. J.; Timken, H. K. C.; Trewella, J. C. U.S. Patent 5639931, 1997.
(20) Barth, J.-O.; Kornatowski, J.; Lercher, J. A. *J. Mater. Chem.* **2002**, *12* (2), 369−373.

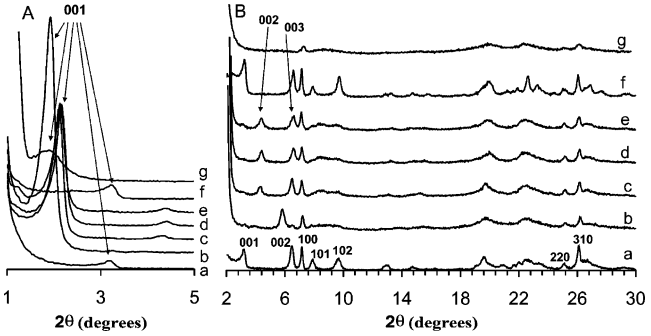

Figure 1. XRD patterns of (a) MCM-22(P); MCM-22(PS-RT) after (b) 10 washes, (c) 20 washes, (d) 30 washes, (e) 40 washes; (f) deswollen material obtained after acidification of MCM-22(PS-RT), (g) MCM-22-(PS-80). Figure 1 has been divided into A and B for better visualization of the 001 peak, and traces have been shifted vertically for the sake of clarity.

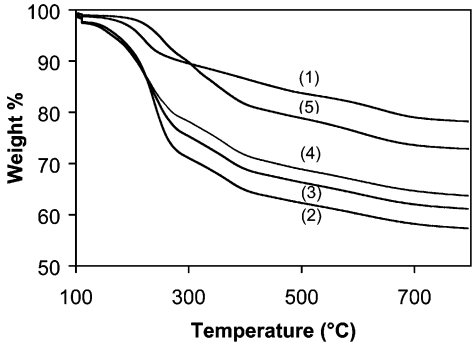

Figure 2. TGA curves for (1) MCM-22(P); MCM-22(PS-RT) after (2) 10 washes, (3) 20 washes, and (4) 40 washes; (5) deswollen material obtained by acidification of MCM-22(PS-RT).

Powder X-ray diffraction (XRD) patterns were collected on a Bruker AXS D5005 diffractometer using Cu Kα radiation to characterize the swelling and pillaring of MCM-22(P). Data were collected in the 2θ range from 0.65° to 30° with a step size of 0.04° and a step time of 3 s.

Thermogravimetric analysis (TGA) was performed to estimate the amount of organic contents in MCM-22(P) and swollen materials. Experiments were carried out under air in the temperature range 110−800 °C (heating rate 10 °C/min) on a Perkin-ElmerTGA-7 analyzer attached to a PC via a TAV7/DX thermal controller.

All NMR spectra were recorded at a field of 9.4 T (BRUKER Avance 400). ^{29}Si MAS NMR spectra were recorded at 79.49 MHz using 7 mm rotors at a spinning speed of 4 kHz, a dwell time of 5 μs, a $\pi/2$ pulse of 3.0 μs, and a recycle delay of 60 s. All spectra were referenced with respect to tetramethylsilane (0 ppm). ^{27}Al MAS NMR spectra were recorded at 104.26 MHz using 4 mm rotors at 12 kHz spinning speed, a dwell time of 2.5 μs, a selective $\pi/6$ pulse of 0.6 μs, and a recycle delay of 1 s. An aqueous solution of aluminum sulfate (0.1 M) was used as the reference (0 ppm). ^{29}Si{^{1}H} CPMAS NMR spectra were acquired using 7 mm rotors at a spinning speed of 4 kHz, a dwell time of 5 μs, a ^{1}H $\pi/2$ pulse of 4.5 μs, high power ^{1}H decoupling, and a recycle delay of 10 s. The Hartmann−Hahn matching conditions were determined using a sample of tetrakis(trimethylsilyl)silane (Si[Si-$(CH_3)_3]_4$).

The crystal morphologies of various materials were examined by scanning electron microscopy (SEM, JEOL 6500) operating at an accelerating voltage of 5 kV. Samples were coated with platinum (50 Å thickness) before imaging.

A FEI Tecnai G2 F30 transmission electron microscope (TEM) equipped with a charge couple device (CCD) and operated at 300 kV was used for direct imaging of various samples. Samples were prepared by sprinkling the powders onto a carbon coated copper grid. For imaging swollen MCM-22(P) from toluene dispersions, a few droplets were placed on a copper grid and allowed to air-dry. For polymer nanocomposites, a JEOL 1210 microscope operating at 120 kV was used for visualization. A Reichert Ultracut S Ultramicrotome equipped with a diamond knife was used for TEM sample preparation to obtain 50−80 nm thick slices of nanocomposite.

Nitrogen adsorption−desorption measurements were carried out at −196 °C on a Autosorb-1 analyzer (Quantachrome Instruments). Prior to measurement, samples were evacuated overnight at 350 °C and 1 mmHg.

3. Results and Discussion

3.1. XRD and TGA. MCM-22(P) has been swollen by CTAB into a highly ordered material and the swelling can be reversed by acidification of the sample. The XRD patterns of MCM-22-(P) before and after swelling and repeated centrifuging/washing are reported in Figure 1. The XRD pattern for MCM-22(P) (Figure 1 trace a) is in agreement with those reported in the literature.[8] Room-temperature swollen MCM-22(P) (MCM-22-(PS-RT)) shows a shift of the 001 peak to lower angles (Figure 1A traces b−e) indicating an increase in layer spacing from 27 Å to about 42 Å. Peaks 220 and 310 are unaffected by swelling, indicating preservation of the crystal structure within the layer. The *hkl* peaks along the *c*-axis (perpendicular to layers) either disappeared or became broader due to the changes in the crystal structure. The 101 and 102 reflections merge together to form a broader peak, as reported previously.[2]

Traces b−e in Figure 1 show the evolution of the swollen structure as a result of repeated washing/centrifuging. The swollen material after 10 cycles of washing (trace b) shows a new peak around a 2θ value of 5.5°. The origin of this peak is not known. Roth and Vartuli[2] report a similar response in swollen MCM-22(P). Further washings resulted in the disappearance of this peak and emergence of two new peaks around 2θ angles of 4.5° and 6.5°. Also, the 001 peak shifts toward slightly higher angles. The two new peaks can be indexed as 002 and 003 based on the position of the 001 peak. These peaks are not present in MCM-22(P) swollen at elevated temperature (MCM-22(PS-80)) (Figure 1, trace g). Also, the peaks are much broader in MCM-22(PS-80), indicating a greater degree of disorder. The room-temperature swelling procedure results in an expanded material with less broadening of peaks as compared to what results when MCM-22(P) is swollen at high temperature. In addition, we obtained 002 and 003 reflections, indicating a long range order of layers in the swollen material. To the best of our knowledge, these reflections have never been reported before in the swollen material and support our claim of a higher degree of ordering as compared to MCM-22(P) swollen at higher temperature.

The TGA curves (Figure 2, traces (2)−(4)) reveal that repeated washings result in a decrease in the organic content in MCM-22(PS-RT), presumably due to removal of CTAB. It seems reasonable to assume that partial removal of CTAB, which might be loosely held in between the layers, results in a more ordered lamellar structure (as evidenced by the emergence of 002 and 003 peaks). This assumption is supported by the slight shift of the 001 peak to larger angles (and hence a decrease in layer spacing as a result of CTAB removal) and the observed reduction in organic content of MCM-22(PS-RT) as a result of repeated washings. We do not completely understand the evolution of structure, viz. the origin and disappearance of the $2\theta = 5.5°$ reflection. However, the XRD pattern of the final swollen structure is well-defined.

Scheme 1. Illustration Showing the Reversible Swelling of MCM-22(P) and Pillaring of the Swollen Material[a]

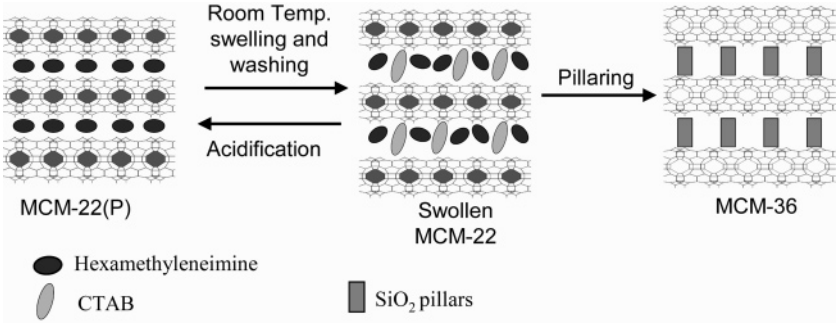

[a] The swollen material can be deswollen back to MCM-22(P) by acidification, suggesting exchange of CTAB surfactant with protons.

3.2. Si/Al Ratio. The pH at the end of the room-temperature swelling procedure was found to be approximately equal to the starting pH of 13.80. On the other hand, the swelling procedures at 80 °C resulted in a significantly lower pH of 12.99. These observations can be explained by comparing the Si/Al ratio of the respective materials. MCM-22(P) had a Si/Al ratio of 46.7 as compared to 43.2 for MCM-22(PS-RT) and 11.8 for MCM-22(PS-80). The decrease in Si/Al ratio as a result of swelling indicates some dissolution of framework silica. The dissolved silica forms monosilicic acid and other oligomeric silicates in the solution, which, on deprotonation, decrease the pH of the solution. Greater dissolution occurs at elevated temperature. Schenkel et al.[15] also report a large reduction in Si/Al ratio, from 33.3 to 20.1, as a result of swelling MCM-22(P) starting with an initial pH of 13.5.

3.3. Reversible Swelling. A remarkable feature of the room-temperature swelling procedure is that the process can be reversed by acidification. Figure 1B (trace f) shows the XRD pattern of the material obtained by acidification of MCM-22-(PS-RT), which appears to be same as that of MCM-22(P). The TGA curve for this material (Figure 2, trace (5)) shows considerably lower organic content than MCM-22(PS-RT), which suggests the removal of CTAB as a result of acidification. The XRD pattern and the TGA analysis suggest that the acidification results in the exchange of CTAB for protons and the layers reassemble to form the MCM-22(P) structure with a characteristic layer spacing of 2.7 nm. The sequence is depicted in Scheme 1. In fact, MCM-22(PS-RT) samples at any stage of washing can be reversed back to the MCM-22(P) structure by suspending them in aqueous solution with pH < 2. Reversibility of the swelling suggests that HMI, initially present in MCM-22(P), most likely remains in between the layers after swelling and directs the reassembly of the layers to the original MCM-22(P) structure upon CTAB removal. However, further investigations are needed to test this hypothesis. Such reversibility does not occur with MCM-22(PS-80), possibly because the layers are broken due to partial dissolution of framework silica. Thus, the resulting material likely has disordered layers that are completely out of registry, which cannot be deswollen back to the MCM-22(P) structure. Instead, ITQ-2 is obtained upon acidification.[8] Further, our preliminary results on swelling MCM-22(P) at various temperatures, ranging from room temperature to 80 °C, suggest that the swelling reversibility behavior changes at a temperature of about 55 °C. At lower temperatures, the swollen material can be restored back to MCM-22(P), while, above this temperature, reversibility is lost. This result is in agreement with our argument that swelling at high temperatures results in partial dissolution of framework silica and destruction of the layered structure which prevents reversibility of the swelling process.

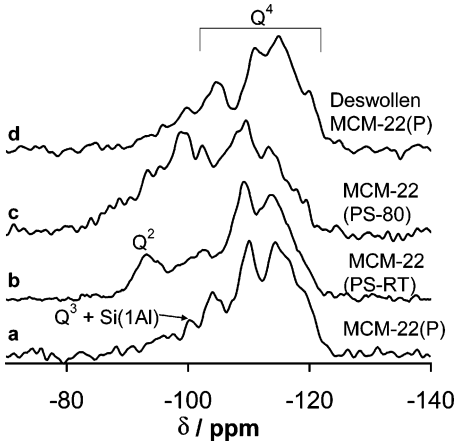

Figure 3. ^{29}Si MAS NMR spectra of (a) MCM-22(P), (b) MCM-22(PS-RT), (c) MCM-22(PS-80), and (d) deswollen MCM-22(P) obtained by acidification of MCM-22(PS-RT).

3.4. Multinuclear Solid-State NMR Investigation. Solid-state ^{27}Al and ^{29}Si MAS NMR and ^{29}Si CPMAS NMR were employed to investigate the structural differences and coordination environment in precursor, swollen, and deswollen MCM-22(P) materials. Figure 3, trace (a), shows a typical ^{29}Si MAS spectrum of MCM-22(P). The main resonances are from silicon atoms coordinated with four silicon atoms (Q^4) due to the low aluminum content of the precursor (Q^n stands for $X_{4-n}Si[OSi]_n$, X = OH or O^- and the expected Si(1Al)/Q^4 ratio ~1:10). Three well-resolved lines, appearing at −104, −110, and −114 ppm, together with two less resolved shoulders at −116.8 and −119 ppm, are attributed to crystallographically nonequivalent framework Q^4 tetrahedral sites (T-sites). These resonances have been tentatively assigned to distinct T-sites by comparing experimental spectra with simulated ^{29}Si MAS NMR spectra of MCM-22 using the Si−O−Si bond angles of the proposed MCM-22 structure.[21−25] The ambiguity in assignment arises due to two possible space groups (*P*6*mmm* and *Cmmm*) that have been

(21) Aiello, R.; Crea, F.; Testa, F.; Demortier, G.; Lentz, P.; Wiame, M.; Nagy, J. B. *Microporous Mesoporous Mater.* **2000**, *35*−*36*, 585−595.
(22) Camblor, M. A.; Corma, A.; Diaz-Cabanas, M.-J.; Baerlocher, C. *J. Phys. Chem. B* **1998**, *102* (1), 44−51.
(23) Kennedy, G. J.; Lawton, S. L.; Rubin, M. K. *J. Am. Chem. Soc.* **1994**, *116* (24), 11000−3.
(24) Lawton, S. L.; Fung, A. S.; Kennedy, G. J.; Alemany, L. B.; Chang, C. D.; Hatzikos, G. H.; Lissy, D. N.; Rubin, M. K.; Timken, H.-K. C.; et al. *J. Phys. Chem.* **1996**, *100* (9), 3788−98.
(25) Vuono, D.; Pasqua, L.; Testa, F.; Aiello, R.; Fonseca, A.; Koranyi, T. I.; Nagy, J. B. *Microporous Mesoporous Mater.* **2006**, *97* (1−3), 78−87.

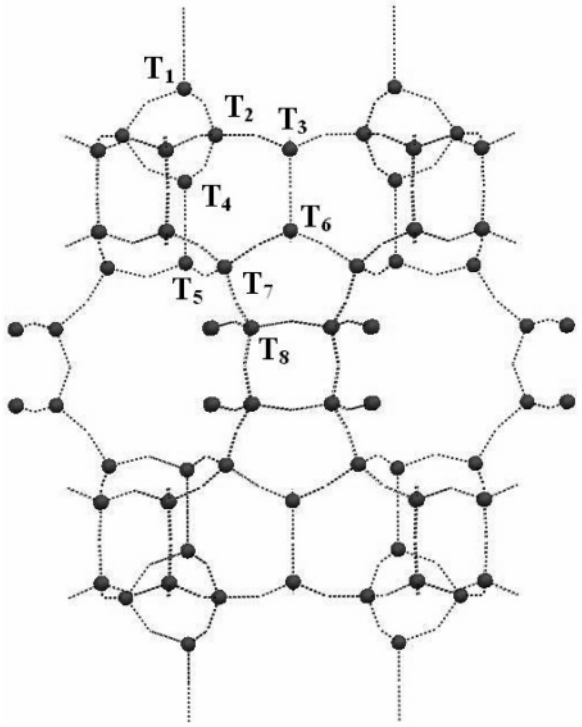

Figure 4. Projection of the MCM-22(P) unit cell indicating the eight crystallographically unequivalent tetrahedral sites.

proposed for MCM-22 based on XRD[26] with each space group having a different number of distinct T-sites. However, the *P*6*mmm* space group has been found to more satisfactorily explain both the ^{29}Si NMR[21,22,24,27] and ^{27}Al NMR[24,28] spectra and the electron diffraction data.[29]

Based on the *P*6*mmm* symmetry, the observed resonances in the ^{29}Si MAS NMR spectra are consistent with the following T-sites (see Figure 4): −104 ppm (T_2), −110 ppm ($T_3 + T_5 + T_4$), −114 ppm (T_8), −116.8 ppm (T_7), and −119 ppm (T_6).[21,22] The line at −100 ppm is due to both Q^3 configuration and the Si(1Al) groups, which appear at the same chemical shift.[30−32] The Q^3 resonances come from the T_1 sites (4 per unit cell) along with certain structural defects which lack connectivity between two Si atoms. Given the high Si/Al ratio of this sample, the Q^3 peak will dominate over the Si(1Al) peak (assuming Q^3 contributions only from the T_1 sites, the expected Si(1Al)/Q^3 ratio will be 1:2.6).

Figure 3, trace b shows the ^{29}Si MAS NMR spectrum for MCM-22(PS-RT). The spectrum is qualitatively very similar to that of MCM-22(P). There is a slight low-field shift of the Q^4 peaks, possibly indicating relaxation of the structure by a reduction of the Si−O−Si bond angles. The primary differences between the two samples are the appearance of a more significant resonance at −93 ppm and the reduction in the intensity of the −116.8 and −119 ppm resonances in the MCM-22(PS-RT) spectra. The −93 ppm peak is assigned to Q^2 groups[17,21,22] and likely arises as a result of breaking some of the Si−O−Si connectivity during swelling. The reduction in the intensity of the −116.8 and −119 ppm resonances suggests there may be some structural changes around T_6 and T_7 sites, which could either be simply a reduction in the Si−O−Si angle, making them indistinguishable from other T-sites, or might be due to bond breaking around T_6 and T_7 sites. However, given that the T_6 and T_7 sites lie well protected inside the layer structure (see Figure 4), these are unlikely to undergo bond breakage during swelling (which is more likely to occur around the T_1, T_2, and T_3 sites, which are near the layer surface). Despite these differences, the overall similarity between the MCM-22-(P) and MCM-22(PS-RT) spectra shows that the precursor has been swollen with minimal change in the local environment of the framework structure. In contrast, MCM-22(PS-80) has a very different spectrum (Figure 3, trace c). There is a significant increase in the spectral intensity between −95 and −105 ppm and a substantial broadening of all resonances suggesting the creation of Q^3 and Q^2 defect sites by breaking Si−O−Si bonds. A decrease in the Si/Al ratio (Si/Al ∼12) implies that Si(1Al) peaks, which appear downfield to the corresponding Q^4 peaks, will also have a significant contribution to the spectra, thereby increasing the overall intensity in this chemical shift range. The overall spectrum of this material suggests an increased dispersion in the local bonding environments.

Figure 3, trace d shows the ^{29}Si MAS NMR spectrum for deswollen MCM-22(P) obtained by acidification of MCM-22-(PS-RT). The spectrum shows re-emergence of −104 and −119 ppm resonances which were present in MCM-22(P) but decreased in intensity after room-temperature swelling (Figure 3, trace b). The spectrum is qualitatively very similar to that of MCM-22(P) and supports the reversibility of the room-temperature swelling procedure as already seen in the XRD patterns of these materials.

The ^{29}Si CPMAS NMR spectra were acquired for all samples to gain further insight into the structural aspects and to distinguish between the Q^3 and Si(1Al) peaks. Two different contact times of 1 and 7 ms were employed. The spectra are shown in Figure 5. For both MCM-22(P) and MCM-22(PS-RT) an increase in the contact time results in a relative increase in the Q^4 resonances due to the increased magnetization transfer (i.e., spin diffusion) observed at longer cross-polarization times, leading to an apparent decrease in the Q^3 and Q^2 signals (compare Figure 5a to 5b and 5c to 5d). At a short contact time (1 ms), the Q^3 and Q^2 species are more rapidly polarized than the Q^4 species because they are in closer proximity to the organic protons and/or silanols.[33] At the longer contact times, the magnetization transfer is more diffuse in that enhancement of all silicon species is observed. Thus, the (apparent) decrease in the −100 ppm peak intensity in MCM-22(P) and MCM-22-(PS-RT) reflects the Q^3 contribution to this peak as suggested earlier. In addition, the spectrum of MCM-22(P) shows a resonance around −94 ppm that was not visible in the corresponding ^{29}Si MAS NMR spectrum (Figure 3, trace a). This resonance is probably due to the presence of a small amount of Q^2 defects in the MCM-22(P) structure, which becomes visible only in the cross polarization (CP) mode. MCM-22(PS-

(26) Leonowicz, M. E.; Lawton, J. A.; Lawton, S. L.; Rubin, M. K. *Science (Washington, DC, United States)* **1994**, *264* (5167), 1910−13.
(27) Camblor, M. A.; Corell, C.; Corma, A.; Diaz-Cabanas, M.-J.; Nicolopoulos, S.; Gonzalez-Calbet, J. M.; Vallet-Regi, M. *Chem. Mater.* **1996**, *8* (10), 2415−2417.
(28) Kennedy, G. J.; Lawton, S. L.; Fung, A. S.; Rubin, M. K.; Steuernagel, S. *Catal. Today* **1999**, *49* (4), 385−399.
(29) Dorset, D. L.; Roth, W. J.; Gilmore, C. J. *Acta Crystallogr., Sect. A* **2005**, *A61* (5), 516−527.
(30) Hunger, M.; Ernst, S.; Weitkamp, J. *Zeolites* **1995**, *15* (3), 188−92.
(31) Kolodziejski, W.; Zicovich-Wilson, C.; Corell, C.; Perez-Pariente, J.; Corma, A. *J. Phys. Chem.* **1995**, *99* (18), 7002−8.
(32) Ma, D.; Deng, F.; Fu, R.; Han, X.; Bao, X. *J. Phys. Chem. B* **2001**, *105* (9), 1770−1779.
(33) Burkett, S. L.; Davis, M. E. *J. Phys. Chem. B* **1994**, *98* (17), 4647−53.

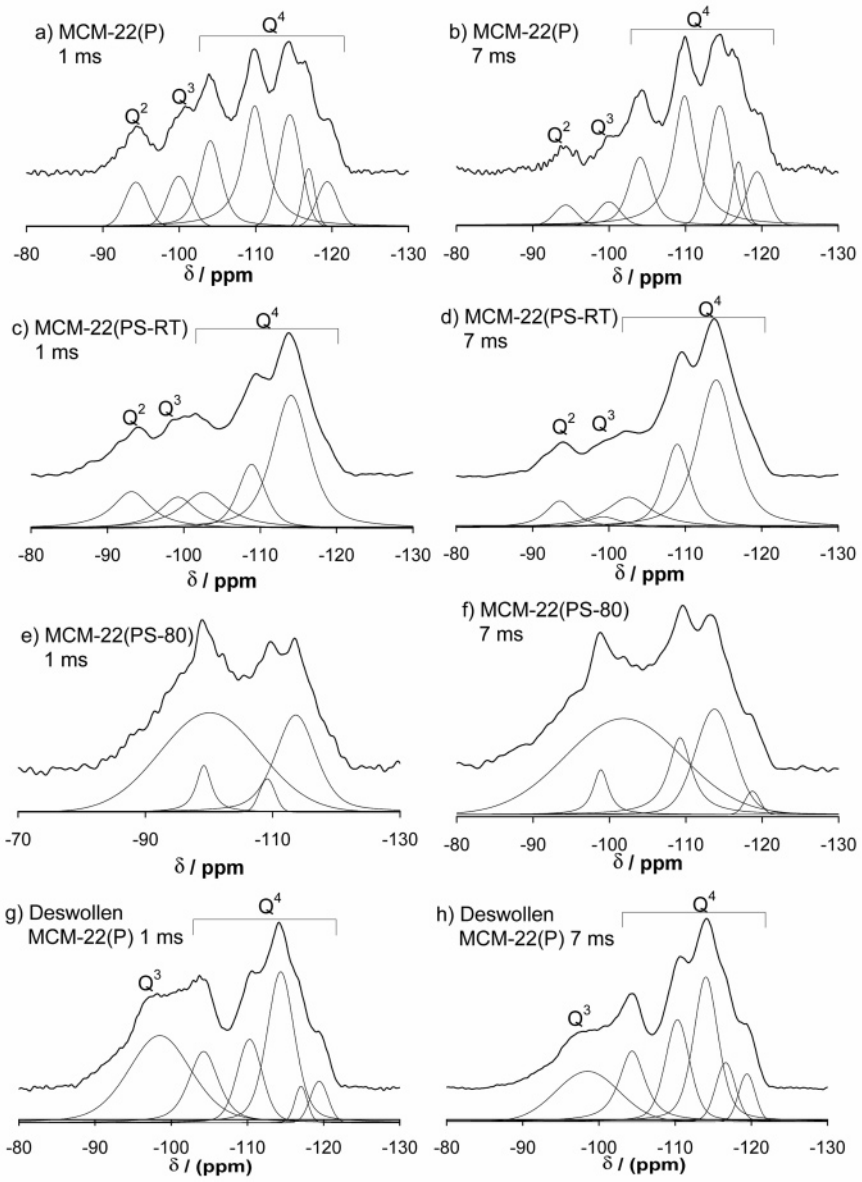

Figure 5. ^{29}Si CPMAS NMR spectra of MCM-22(P) (a) contact time 1 ms, (b) contact time 7 ms; MCM-22(PS-RT) (c) contact time 1 ms, (d) contact time 7 ms; MCM-22(PS-80) (e) contact time 1 ms, (f) contact time 7 ms; and deswollen MCM-22(P) (g) contact time 1 ms, (h) contact time 7 ms. In each figure, the top curve represents the spectra obtained experimentally and bottom curves represent the deconvolution into individual peaks.

80) shows a large contribution from a very broad peak centered around −100 ppm (Figure 5e and 5f). This contribution is expected for two reasons: Q^3 species created as a result of swelling and, increased dominance of the Si(1Al) peak as a result of a decreased Si/Al ratio. The ^{29}Si CPMAS NMR of deswollen MCM-22(P) with a 1 ms contact time (Figure 5g) shows a substantial enhancement of the resonances from −90 to −100 ppm, indicating selective magnetization transfer. This is much more pronounced in the deswollen sample as compared to the MCM-22(PS-RT) or MCM-22(P). A likely explanation for this could be that, at the high pH (13.8) used for swelling, many of the silanol groups become deprotonated and, upon acidification, they become reprotonated.

The ^{27}Al NMR spectra for various materials are shown in Figure 6. All four materials show two peaks around 50 and 56 ppm, consistent with previous reports.[24,28,30,31] These peaks have been assigned to two different sets of T-sites, differentiated by location in the framework.[28,31] Kennedy et al.[28] used the Si−O−Al bond angles obtained from the structure of MCM-22 to calculate the chemical shifts of various T-sites. By comparing calculated chemical shifts to experimentally observed shifts, the

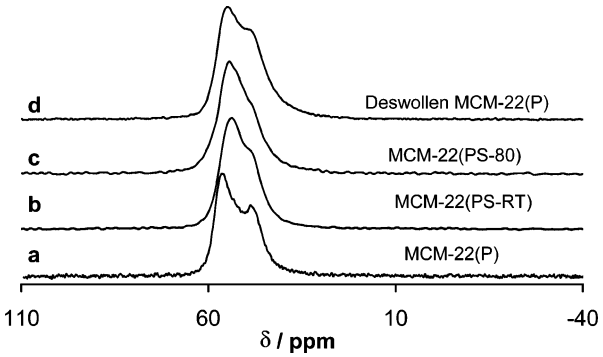

Figure 6. ^{27}Al MAS NMR spectra of (a) MCM-22(P), (b) MCM22 (PS-RT), (c) MCM-22(PS-80), and (d) deswollen MCM-22(P) obtained by acidification of MCM-22(PS-RT).

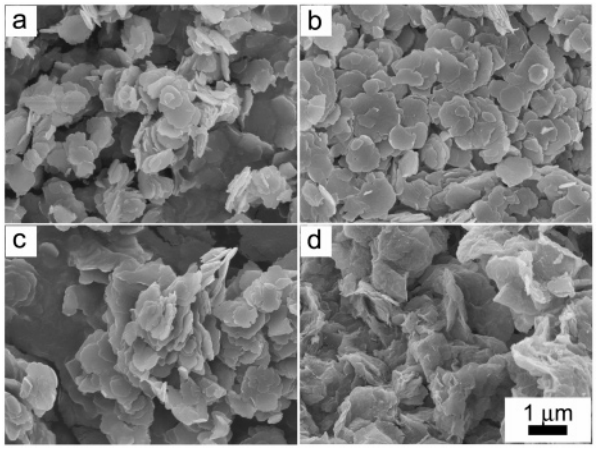

Figure 7. SEM images of (a) MCM-22(P), MCM-22(PS-RT) after (b) 10 washes, (c) 40 washes, (d) MCM-22(PS-80).

T_6 and T_7 sites were assigned to the 50 ppm resonance and all the other T-sites to the 56 ppm resonance. Swelling MCM-22-(P) results in the reduction of the 50 ppm peak intensity (Figure 6, traces b and c), which suggests some structural changes around the T_6 and T_7 sites. This observation is in agreement with the ^{29}Si MAS NMR results, which also indicated structural changes around these T-sites. Overall, the NMR spectrum of MCM-22(PS-RT) more closely resembles the one obtained from MCM-22(P) as opposed to the one derived from MCM-22(PS-80). Deswollen MCM-22(P) (Figure 6, trace d) has a spectrum similar to those obtained from MCM-22(PS-RT) and MCM-22(P) materials, indicating a close structural relationship between the three materials.

Based on the ^{29}Si MAS NMR and the ^{27}Al NMR results, we conclude that swelling MCM-22(P) at room temperature largely preserves the layer structure, in contrast to the significant structural disruptions that occur at 80 °C. Room-temperature swelling does lead to certain specific structural differences, around T_6 and T_7 sites, which may reflect a reduction in the average Si−O−Si bond angle at these sites.

3.5. Electron Microscopy. SEM images obtained from the precursor and swollen materials are shown in Figure 7. The MCM-22(P) crystals (Figure 7a) are thin rounded flakes, less than a micron in diameter. Swelling at room temperature, and 10 and 40 subsequent washes, does not result in any significant changes in the crystal morphology as evidenced by comparing Figure 7a−c; recall, however, differences in the XRD patterns (Figure 1, trace b and trace e) noted earlier. Swelling at an elevated temperature does produce significant morphological changes as shown in Figure 7d. The crystals no longer have sharp edges and appear to be highly curled and broken. This is likely due to the dissolution of framework silica.

Figure 8 shows low magnification TEM images of various samples. MCM-22(P) has a thin flake-like morphology (Figure 8a) with layers stacked over each other in a lamellar arrangement (Figure 8b). Swelling at room temperature does not lead to any major changes in the particle morphology, as already seen by SEM and further shown by a TEM micrograph in Figure 8c. In contrast, Figure 8d, which shows the morphology of the material swollen at 80 °C, clearly shows the loss of lamellar morphology and crystal facets. Layers appear to be curled, partially delaminated, and out of registry.

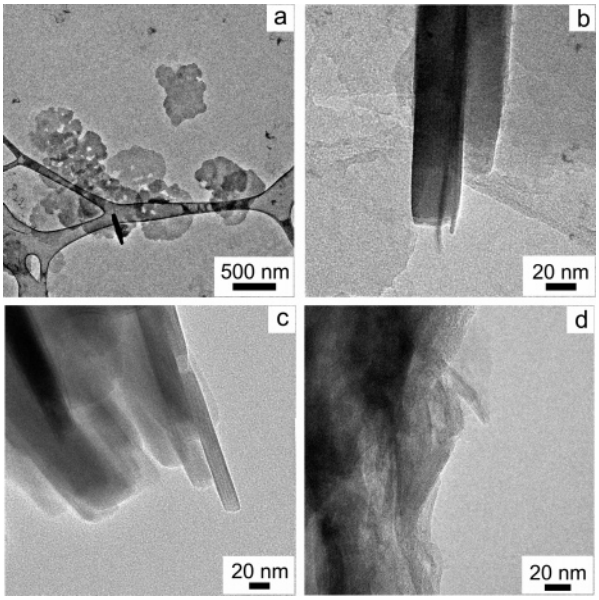

Figure 8. TEM images of (a) MCM-22(P) perpendicular to layer thickness, (b) MCM-22(P) edge-on view, (c) MCM-22(PS-RT), and (d) MCM-22-(PS-80).

High-resolution TEM (HRTEM) was used to examine the structure of individual layers and the associated gallery spacing. Figure 9 shows TEM micrographs for various specimens. Structural schematics of MCM-22(P) have been overlaid on the TEM micrographs in order to guide visualization. MCM-22(P) (Figure 9a) shows ∼2.5 nm thick layers. Each layer appears as two dark bands separated by a bright band. The bright band is attributed to the 10-MR pore system within the layer, while the dark bands appear due to the higher silica density in the remaining parts of the layer (top and bottom). The gallery space between the two layers also appears as a bright band. MCM-22(PS-RT) (Figure 9b) displays well ordered layers with an expanded interlayer distance relative to MCM-22(P). Shown in Figure 9c is a TEM image of the material obtained by acidification of MCM-22(PS-RT). This image shows the layer spacing and structure corresponding to MCM-22(P) and is consistent with Figure 9a. This provides another piece of evidence, in addition to XRD, for the reversible swelling of MCM-22(P) at room temperature. TEM images of MCM-22-(PS-80) are shown in Figure 9d−f. MCM-22(PS-80) shows a different morphology than MCM-22(PS-RT). Here, crystals appear to be much more fragmented, with curled layers and amorphous regions. As evidenced by Figure 9d and 9e, the layers generally lack the long range ordered stacking obtained for MCM-22(PS-RT). Figure 9e shows a swollen particle with a part containing well resolved layers and another part that looks amorphous. Although some ordered layers with increased interlayer spacing were observed (Figure 9f), such regions make up a minor fraction of the specimen examined. We conclude that the hot basic conditions used for swelling the sample partly degrade the structure and dissolve the framework silica in some regions.

3.6. Pillaring of Swollen Materials. The swollen zeolite materials can be pillared to make MCM-36 (see Scheme 1). Figure 10a illustrates an XRD pattern obtained after pillaring MCM-22(PS-RT). This pattern is characteristic of an MCM-36 material with an intense low angle 001 peak at the 2θ value

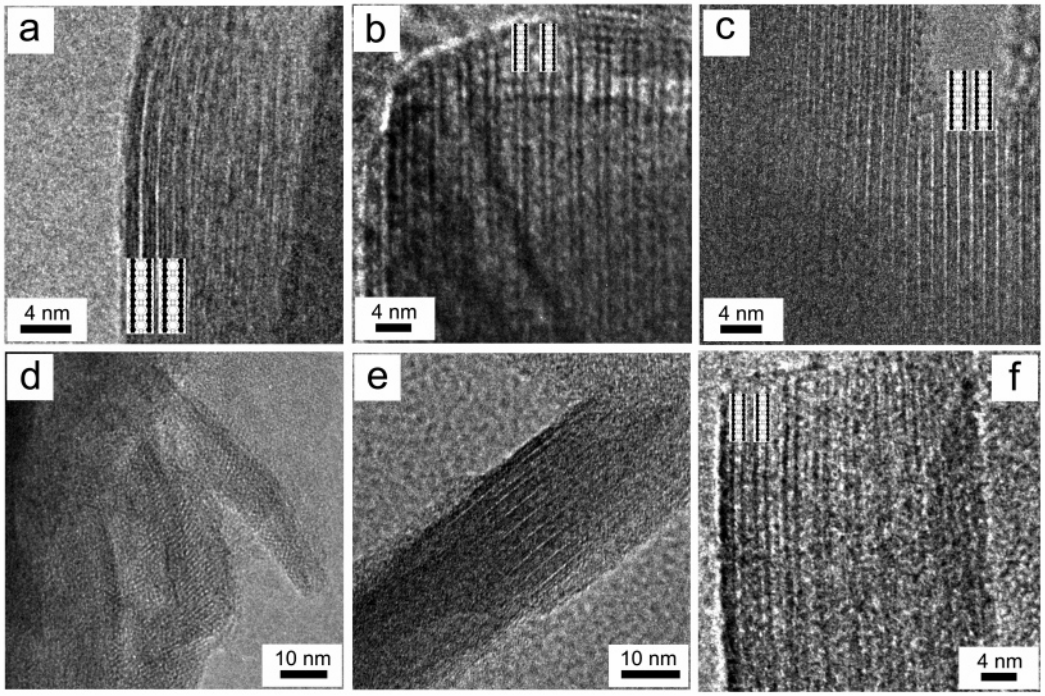

Figure 9. HRTEM images of (a) MCM-22(P), (b) MCM-22(PS-RT), (c) deswollen MCM-22(P) obtained by acidification of MCM-22(PS-RT), and (d−f) MCM-22(PS-80). Schematics of single MCM-22(P) layer have been overlapped on some of the images to facilitate identification of layers.

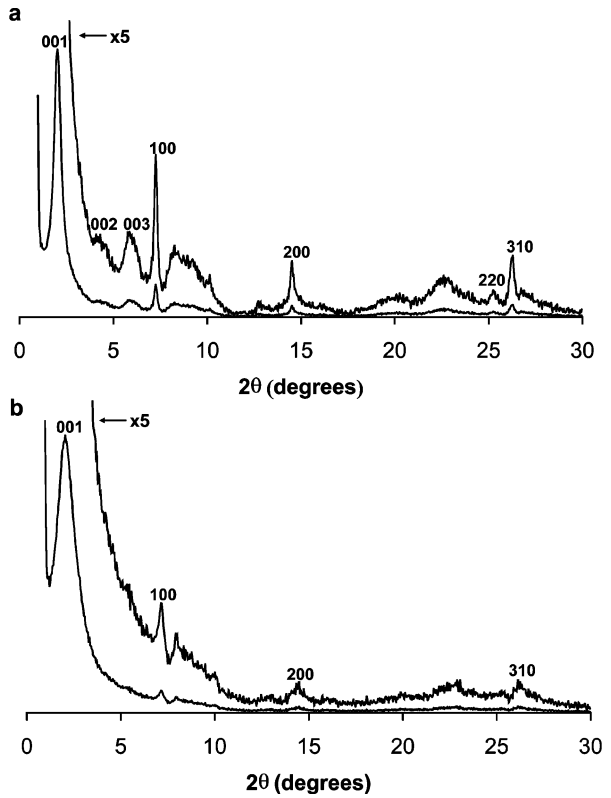

Figure 10. XRD pattern of MCM-36 obtained by pillaring (a) MCM-22-(PS-RT) and (b) MCM-22(PS-80). Second curve in each figure is a 5 times magnification of lower curve for better visualization of peaks.

of 2°.[6,34,35] Remarkably, the 002 and 003 reflections are plainly visible, features that have never been reported for MCM-36 to the best of our knowledge. The presence of these reflections indicates that the material retains long range order even after pillaring. Figure 10b shows the pillared material obtained from MCM-22(PS-80). The XRD pattern is grossly similar to that of the MCM-36 analogue obtained from MCM-22(PS-RT), except that the peaks are broader and the 002 and 003 reflections are not visible indicating the absence of long range order.

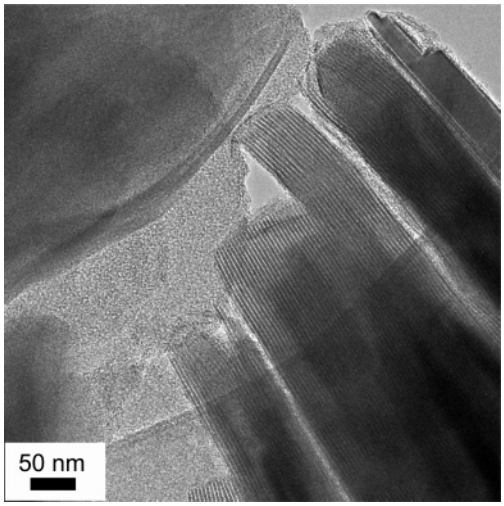

Figure 11. TEM image showing MCM-36 analogue obtained by pillaring MCM-22(PS-RT).

Figure 11 shows a TEM image of the MCM-36 analogue obtained by pillaring MCM-22(PS-RT). This material shows regularly spaced layers (dark lines) with an interlayer distance of l_{TEM} = 42 Å, which agrees well with the XRD value, l_{XRD} = 44 Å.

Nitrogen adsorption experiments further confirm successful pillaring. Figure 12 shows the nitrogen adsorption/desorption curves for MCM-22 and the MCM-36 analogue obtained from MCM-22(PS-RT). For the MCM-36 analogue, the increase in

(34) He, Y. J.; Nivarthy, G. S.; Eder, F.; Seshan, K.; Lercher, J. A. *Microporous Mesoporous Mater.* **1998**, *25* (1−3), 207−224.
(35) Roth, W. J.; Kresge, C. T.; Vartuli, J. C.; Leonowicz, M. E.; Fung, A. S.; McCullen, S. B. *Stud. Surf. Sci. Catal.* **1995**, *94*, 301−8.

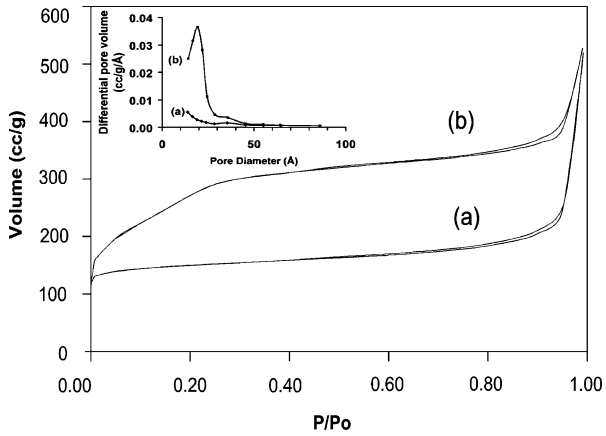

Figure 12. N_2 adsorption/desorption isotherm and BJH pore size distribution (Inset) of (a) MCM-22 and (b) MCM-36 analogue obtained by pillaring MCM-22(PS-RT).

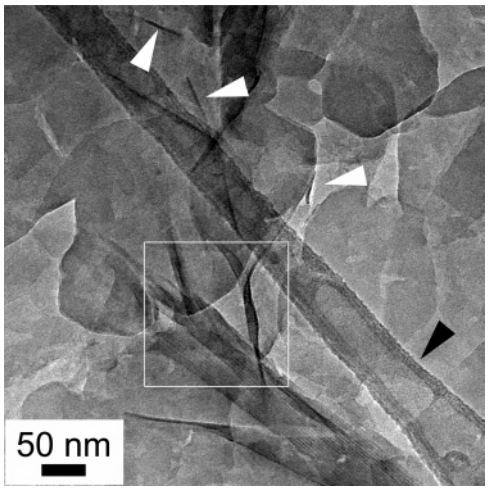

Figure 13. TEM image of the dispersion of MCM-22(PS-RT) in toluene. Sample was prepared by drying a few drops of dispersion onto a microscope grid.

adsorption up to a relative pressure (P/P_0) of 0.4 clearly indicates the presence of mesoporosity created by pillaring. MCM-22, on other hand, saturates at a relative pressure of 0.1. The BET surface area of the pillared material was found to be 934 m^2/g, which is significantly higher than the value 560 m^2/g obtained for MCM-22. These surface area values compare well with those reported in the literature[17,34] (400−500 m^2/g for MCM-22 and 800−950 m^2/g for MCM-36). The BJH pore size distribution (Figure 12 inset) also shows a substantial increase in mesopore volume (15−35 Å) as a result of pillaring. Successful preparation of the pillared MCM-36 material independently corroborates our conclusion regarding swelling at room temperature drawn from XRD and TEM.

Unlike the high-temperature swollen MCM-22(P), the room-temperature swollen material cannot be exfoliated simply by ultrasonication in water to produce ITQ-2.[8] This suggests that the high-temperature swelling of MCM-22(P) and subsequent ultrasonication to produce ITQ-2 is essentially a fragmentation process resulting in exfoliated and other fragments. Room-temperature swelling, on the other hand, results in highly ordered material, without fragmentation. The interlayer forces are still strong enough to prevent exfoliation by ultrasonication.

3.7. Polystyrene-Swollen MCM-22 Nanocomposites. Polystyrene-MCM-22(PS-RT) nanocomposites were prepared by solvent casting and melt blending techniques. For solvent casting, toluene was found to be a suitable solvent to disperse the swollen material based on the optical clarity of the dispersion. Figure 13 shows a TEM image obtained by drying a few drops of the toluene dispersion. A few exfoliated single layers (indicated by white arrows) are visible. The area marked by the white box on the image shows a crystal in the process of exfoliation (as seen by the curving and detachment of layers). The feature from the carbon on the microscope grid has been indicated by a black arrow to distinguish it from the sample. XRD data (not shown here) indicates that solvent intercalation results in further expansion of interlayer distances and that subsequent ultrasonication results in partial exfoliation.

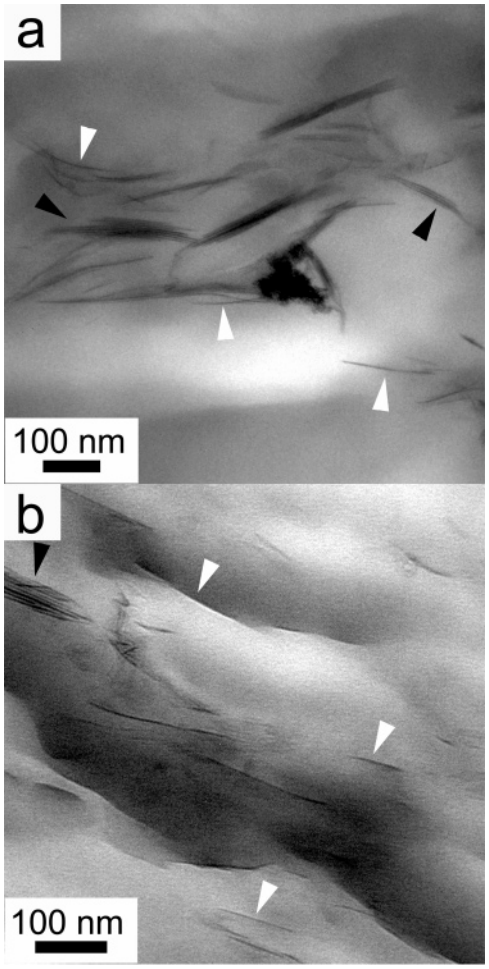

Figure 14. TEM images of polystyrene-MCM-22(PS-RT) nanocomposite prepared by (a) solvent casting and (b) melt compounding.

Figure 14a shows a TEM micrograph of the polystyrene-MCM-22(PS-RT) nanocomposite prepared from solvent casting. Many single exfoliated layers (some indicated by white arrows) can be seen along with fewer partially exfoliated and intercalated layered structures (some indicated by black arrows). Figure 14b shows a TEM micrograph of the nanocomposite prepared by the melt compounding technique. It shows a lot of individual exfoliated layers (some indicated by white arrows) along with a polymer-intercalated stack-of-layers (indicated by a black arrow). Apparently, the shear stress generated during the melt compounding causes the slipping of layers and eventually forces them apart.[36] These images clearly demonstrate the feasibility of the concept of polymer-exfoliated-MCM-22 nanocomposites.

Further work to increase the extent of exfoliation and evaluate performance in membrane and other applications is underway.

4. Conclusion

A procedure has been demonstrated for swelling MCM-22-(P) layers without degradation of the in-plane layer morphology. MCM-22(P) can be swollen under high pH conditions at room temperature. The resulting material evolves to a highly ordered structure with increased layer spacing on repeated washings with water. The swollen material can be successfully pillared to produce an MCM-36 analogue which retains layers with composition and structure closer to those present in MCM-22-(P). An interesting feature of the swollen material is that it can be reversibly deswollen back to MCM-22(P) by acidification. This is in contrast to the material produced by high-temperature swelling process that upon acidification leads to ITQ-2 and is attributed to the preservation of the layer structure. This swelling procedure is well suited for polymer nanocomposite and thin coating fabrication, which requires swelling of MCM-22(P) layers with retention of crystal structure to maintain the high aspect ratio of the layers. The preliminary work on polymer nanocomposites using the swollen material reveals the partially exfoliated morphology of MCM-22 layers in a polymer matrix.

Acknowledgment. This work was made possible with the financial support from the NSF (CBET-0403574 (NIRT) and 0327811) and DOE (Award No. DE-FG26-04NT42119). Parts of this work were carried out in the University of Minnesota I.T. Characterization facility, which receives partial support from the NSF through the NNIN program. D.F.S. and E.J. acknowledge the Donors of the American Chemical Society Petroleum Research Fund for partial support of this research (Grant 43942-AC10).

JA077711I

(36) Fornes, T. D.; Yoon, P. J.; Keskkula, H.; Paul, D. R. *Polymer* **2001**, *42* (25), 09929−09940.